Structure
Article

The Molecular Mechanism of Toxin-Induced Conformational Changes in a Potassium Channel: Relation to C-Type Inactivation

Ulrich Zachariae,[1,2] Robert Schneider,[3] Phanindra Velisetty,[4] Adam Lange,[3] Daniel Seeliger,[1] Sören J. Wacker,[1] Yasmin Karimi-Nejad,[5] Gert Vriend,[2] Stefan Becker,[3] Olaf Pongs,[4] Marc Baldus,[3] and Bert L. de Groot[1,*]
[1]Computational Biomolecular Dynamics Group, Max Planck Institute for Biophysical Chemistry, Am Fassberg 11, 37077 Göttingen, Germany
[2]Centre for Molecular and Biomolecular Informatics, Nijmegen Centre for Molecular Life Sciences, Radboud University Nijmegen, P.O. Box 9010, 6500 GL Nijmegen, The Netherlands
[3]Department of NMR-Based Structural Biology, Max Planck Institute for Biophysical Chemistry, Am Fassberg 11, 37077 Göttingen, Germany
[4]Zentrum für Molekulare Neurobiologie, Institut für Neurale Signalverarbeitung, Universität Hamburg, Falkenried 94, 20251 Hamburg, Germany
[5]Solvay Pharmaceuticals GmbH, Hans-Böckler-Allee 20, 30173 Hannover, Germany
*Correspondence: bgroot@gwdg.de
DOI 10.1016/j.str.2008.01.018

SUMMARY

Recently, a solid-state NMR study revealed that scorpion toxin binding leads to conformational changes in the selectivity filter of potassium channels. The exact nature of the conformational changes, however, remained elusive. We carried out all-atom molecular dynamics simulations that enabled us to cover the complete pathway of toxin approach and binding, and we validated our simulation results by using solid-state NMR data and electrophysiological measurements. Our structural model revealed a mechanism of cooperative toxin-induced conformational changes that accounts both for the signal changes observed in solid-state NMR and for the tight interaction between KcsA-Kv1.3 and Kaliotoxin. We show that this mechanism is structurally and functionally closely related to recovery from C-type inactivation. Furthermore, our simulations indicate heterogeneity in the binding modes of Kaliotoxin, which might serve to enhance its affinity for KcsA-Kv1.3 further by entropic stabilization.

INTRODUCTION

Potassium channels are tetrameric membrane proteins that selectively pass K^+ ions across the plasma membrane (Roux, 2005; Hille et al., 1999). They play a crucial role in the control of the electrochemical potential of all living cells. Voltage-gated K^+ channels (Kv channels) generate electrical impulses in nerve, muscle, and endocrine cells, and they open or close in response to changes in the transmembrane voltage, sensed by their voltage-sensing domains (Long et al., 2005; Yellen, 2005). With regard to structure, the most extensively studied potassium channel is KcsA from the prokaryote *Streptomyces lividans*. Its high-resolution X-ray structure provides a detailed picture of a potassium channel and its selectivity filter (Zhou et al., 2001). Molecular dynamics (MD) studies revealed the mechanism of K^+ permeation and the energetic basis for ion selectivity (Bernèche and Roux, 2001; Åqvist and Luzhkov, 2000; Shrivastava and Sansom, 2000). KcsA lacks a canonical voltage-sensing domain and is gated by pH. Unexpectedly, its conductivity has recently been found to be strongly coupled to voltage changes across the membrane (Cordero-Morales et al., 2006a, 2006b, 2007).

Scorpion toxins are polypeptides of ~35–40 amino acids that exert their toxic effect by binding to the extracellular side of potassium channels, thereby blocking ion conduction (Hidalgo and MacKinnon, 1995; Aiyar et al., 1995). Related peptides are found as the major toxic agents in the venoms of spiders, snakes, and sea anemone. The affinities between these peptidic toxins and potassium channels are among the strongest of all known protein-protein complexes (Garcia et al., 2001). Kaliotoxin (KTX), a 38 residue toxin from the scorpion *Androctonus mauretanicus mauretanicus*, specifically blocks the voltage-gated K^+ channel Kv1.3. KTX contains an α helix and two antiparallel β strands that are connected by three disulfide bonds (Lange et al., 2006). It has been shown to bind to a KcsA-Kv1.3 chimera with an affinity of 30 pM (Lange et al., 2006; Aiyar et al., 1995). Although a large number of experimental and theoretical studies have been carried out to address the interaction between toxin peptides and potassium channels, atomic structures of these tight complexes are not available yet.

The most detailed information on the structure of channel-toxin complexes comes from computational studies (Eriksson and Roux, 2002), double mutant binding cycles (Ranganathan et al., 1996), and a recent solid-state NMR (ssNMR) study by Lange et al. (2006). The double mutant cycles showed major residues of the extracellular surface of the Shaker K^+ channel that are involved in the interaction with Agitoxin2 (Ranganathan et al., 1996). In addition, the ssNMR experiment revealed that KTX binding to the KcsA-Kv1.3 chimera changes the conformational states of both KTX and the channel. Based on an analysis of chemical-shift perturbations, it was shown that toxin binding does not simply block the channel entrance, but is also accompanied by a conformational change in the selectivity filter of the

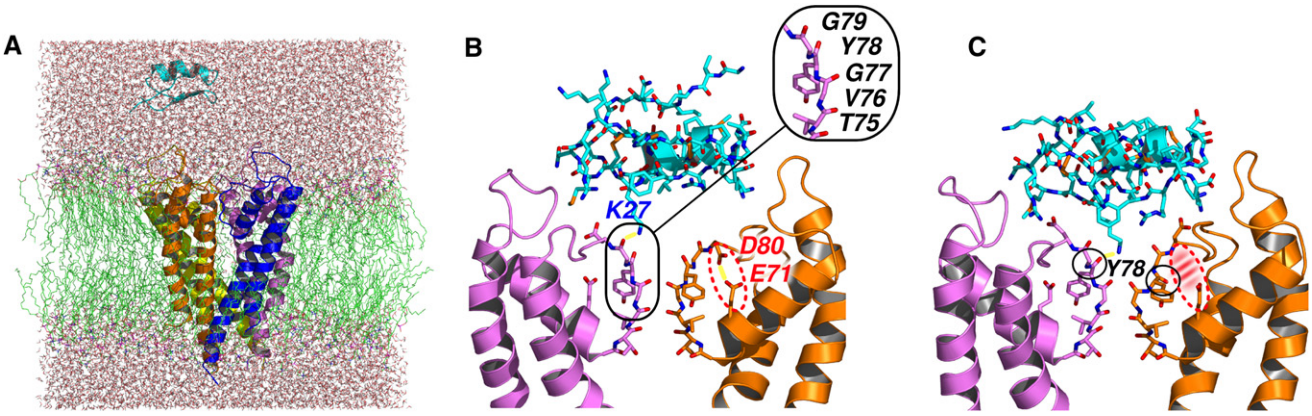

Figure 1. KTX Binding to KcsA-Kv1.3

(A) Molecular system showing the starting configuration for the MD simulation of spontaneous KTX binding to KcsA-Kv1.3 immersed in a membrane bilayer.

(B) Encounter complex formed by KTX and the extracellular surface of KcsA-Kv1.3. The selectivity filter region of one subunit (Thr75-Gly79) is highlighted in the top-right box. The hydrogen bond between KTX Lys27 and KcsA-Kv1.3 Gly79 (purple chain) and the hydrogen bond between KcsA-Kv1.3 Asp80 and Glu71 (orange chain) are shown in yellow. In the purple chain, this hydrogen bond was disrupted spontaneously upon KTX approach.

(C) Conformational change of Asp80 upon deprotonation of Glu71 (orange chain, subunit 3, residue assignments are as in [B]). The side chain of Asp80 flips toward the molecular surface and forms a salt bridge with KTX, leaving a cavity in KcsA-Kv1.3 next to the selectivity filter (red shaded area). The backbone carbonyl moiety of Tyr78 flips into this cavity (orange chain), when it is not bound to KTX Lys27 (purple chain).

channel (Lange et al., 2006). The largest backbone chemical-shift changes were observed for the residues Gly77, Gly79, and Tyr78, which are located in the extracellular entrance of the selectivity filter. The largest side chain chemical-shift changes were observed for Glu71 and Asp80, which are both located directly adjacent to the selectivity filter. The molecular mechanism underlying these chemical-shift changes has hitherto remained elusive.

An important question arising from the ssNMR study of the KTX:KcsA-Kv1.3 complex was why the four channel subunits gave rise to a single ssNMR signal set in spite of tight binding of the nonsymmetric toxin peptide (Lange et al., 2006). This symmetry cannot easily be explained by the four-fold symmetry of the channel, since contacts between specific residues from KTX and specific channel subunits, stable during the timescale of the NMR experiment, would have been expected to distinguish these subunits from the remaining ones, regardless of which chain is involved.

The results of the ssNMR study (Lange et al., 2006) raised the question of why a protein-protein interaction of very high affinity is accompanied by significant structural changes. The adoption of an induced conformation by complex formation is considered to cost energy and decrease the overall affinity (Tobi and Bahar, 2005; Goh et al., 2004). Moreover, in all cases, the decrease of conformational freedom upon complexation could be expected to lead to an entropic penalty, reducing the affinity. Recently, however, Frederick et al. (2007) demonstrated that the conformational entropy of proteins can lower or eliminate this entropic penalty in some cases, and thereby significantly facilitate high-affinity interactions.

We have studied the structural changes elicited by KTX binding to the KcsA-Kv1.3 channel by using atomistic MD simulations, electrophysiological measurements, and ssNMR data. The unbiased MD simulations spontaneously spanned the complete pathway of toxin approach and binding. We present an atomistic model of the KTX complex of KcsA-Kv1.3, in which specific conformational changes around the selectivity filter region are observed that are consistent with the chemical-shift changes observed in ssNMR. These conformational changes are closely related to recovery from C-type inactivation (Cordero-Morales et al., 2006a, 2006b, 2007). C-type inactivation is a structural mechanism that leads to a time-dependent loss of channel conductivity after channel opening and takes place at the extracellular entrance of the K^+ channel (Cordero-Morales et al., 2006a, 2006b, 2007). Our electrophysiological experiments confirm that binding of KTX is indeed sensitive to the C-type inactivation state of Kv1.3.

RESULTS

An Atomistic Structural Model of the KTX-KcsA-Kv1.3 Complex

Eight simulations, each covering 10 ns, were performed on KcsA-Kv1.3 embedded in a POPC membrane with different random initial positions of KTX in the extracellular bulk phase. The initial distance from the KTX Lys27 side chain to the entrance of the selectivity filter was larger than 25 Å in each simulation. No bias or artificial driving force was applied. All of these simulations showed strong attraction between the channel and the toxin. Spontaneous and stable toxin binding of KTX to the selectivity filter of the channel was observed in three simulations. Of these, the simulation that showed binding of KTX Lys27 closest to the original extracellular S0 potassium-binding site (Zhou et al., 2001) was chosen for further detailed analysis. This binding site is formed by the four Gly79 carbonyl oxygen atoms at the entrance to the selectivity filter. The side chain nitrogen atom of Lys27 formed a hydrogen bond to the Gly79 of one of the subunits (Figure 1B). The binding of Lys27 to the selectivity filter that was observed to occur spontaneously in the simulation is in agreement with previous suggestions made on the basis of

double mutant cycles, electrophysiological studies, and docking calculations (Eriksson and Roux, 2002; MacKinnon et al., 1998; Ranganathan et al., 1996). In addition, strand β2 of KTX was found to form the main interaction surface with the channel, in agreement with previous double mutant cycle experiments (Ranganathan et al., 1996).

Alterations in the Protonation State of the Glu71/Asp80 Pair

Subsequently, we analyzed specific channel residues of the interaction surface of the complex in detail. Significant chemical shift changes were observed in the ssNMR experiment (Lange et al., 2006) for the side chains of Asp80 and Glu71 upon KTX binding. Previous studies reported that the carboxyl-carboxylate interactions between these two residues influence the conformation of the selectivity filter (Luzhkov and Åqvist, 2000; Bernèche and Roux, 2002) and confer stability to the channel (Choi and Heginbotham, 2004). We started our simulations from a state in which Glu71 was protonated, as previously reported (Bernèche and Roux, 2002). The side chain of Asp80 frequently rotates away from the protonated Glu71 and points toward the molecular surface of KTX (Figure 1B, purple chain). This motion is favored by the presence of the highly positively charged (+5e) KTX.

A recent quantum chemical study reported only a slightly higher protonation probability for Glu71 compared to a protonated, unflipped Asp80 side chain (Bucher et al., 2007), and recent experimental findings by mutation studies and electrophysiology (Cordero-Morales et al., 2006b) suggest that the Glu71 side chain is not permanently protonated. In light of the ssNMR results showing substantial chemical-shift changes for both residues upon KTX binding, we studied the effects of side chain protonation states of Glu71 and Asp80 with respect to binding of KTX. The flipped Asp80 side chain is likely deprotonated, and with the Asp80 not nearby, protonation of Glu71 seems rather unfavorable.

The newly introduced protonation scheme with both Glu71 and Asp80 deprotonated led to a fast rotation of all four Asp80 side chains to the surface where they interact with the toxin (Figure 1C). This rotation resulted in a distortion of the entrance region of the selectivity filter (Gly77 to Gly79) and created in each subunit a cavity next to the selectivity filter (red shaded area in Figure 1C). In the toxin-bound state, salt bridges and hydrogen bonds were formed between all Asp80 side chains and basic or polar residues of the toxin. The formation of intimate contacts between Asp80 and the toxin stabilized the bound state of the toxin. As a result, the side chain of KTX Lys27 was drawn ~4 Å deeper into the selectivity filter, and it was bound to the carbonyl oxygen of Tyr78 (Figure 1C). Complete block of potassium ion conduction is not likely before the solvation shell is disrupted, allowing for a tightened stage of association (Figures 1B and 1C).

To further investigate the protonation state of the Glu71/Asp80 pair in the KTX-bound state, we tested the effect of the reprotonation of Glu71. In a simulation of 10 ns, the KTX:KcsA-Kv1.3 complex was destabilized by this change, and the Lys27 side chain returned to its initial position, bound to a carbonyl oxygen of Gly79. Subsequently, the observed backbone conformational changes in the selectivity filter region were reversed. This latter observation is not compatible with the ssNMR data shown below; thus, it seems most likely that both Asp80 and Glu71 are charged in the KTX complex.

ssNMR Data Are Consistent with Conformational Changes Observed in the MD Structural Model

We performed ssNMR experiments on the KTX:KcsA-Kv1.3 complex to validate the conformational changes observed in the MD simulations. The conformational change of the Asp80 side chains in the MD simulation triggered subsequent conformational changes in the selectivity filter of KcsA-Kv1.3. Tyr78 was the only residue in the selectivity filter that showed large φ/ψ changes during the simulation with bound KTX (see Figure 3A). Figure 1C (orange chain) shows that Tyr78 underwent a backbone flip that caused its carbonyl oxygen atom to point into the cavity originally occupied by the Asp80 side chain. The flip is seen in two subunits. In the other two subunits, in which the Tyr78 carbonyl oxygen forms hydrogen bonds to the KTX Lys27 side chain, this flip is not observed; however, an increase in the local conformational flexibility was observed (e.g., Figure 1C, purple chain).

We crossvalidated our simulation results by calculating the potential influence of the backbone flip on the expectation value for the ^{13}C chemical shift for each frame of the simulation trajectory by using the SHIFTX software (Neal et al., 2003). The results were compared to the chemical shifts measured by ssNMR. The C_α chemical shift of Tyr78 was particularly affected by toxin binding in the ssNMR experiment (Lange et al., 2006). Figure 2B shows that the backbone flips led to a remarkable deviation of the calculated chemical shift for KcsA-Kv1.3 from the starting configuration. The change occurred after ~3.5 ns and split the original signal from a unimodal chemical-shift distribution with a maximum at δ = 60.2 ppm to a bimodal distribution of signals with separated contributions at δ = ~56 ppm and δ = ~58–60 ppm. The most striking change is the new signal at δ = ~56 ppm (Figure 2B), which originates from the two Tyr78 residues undergoing the backbone flip. This shift change strongly correlates with the observed ψ angle transitions at Tyr78 in two subunits. The remaining two subunits stably bind the side chain of Lys27.

We compared the data derived from the simulations of the complex with simulations of the unbound KcsA-Kv1.3 channel. In the latter simulations, the side chains of Glu71 were assumed to be protonated and Asp80 unflipped, i.e., bound to this protonated Glu71. The calculated C_α chemical shift of Tyr78 remains at ~60 ppm here and shows no change, in accordance with the absence of a backbone flip (Figure 2C). Accordingly, the calculated and measured upfield shift of the C_α signal of Tyr78 is a KTX-induced effect, resulting from the rotation of the Tyr78 backbone in the KTX-bound structure.

Figure 3A shows a section of a two-dimensional (^{15}N,^{13}C) ssNMR correlation spectrum highlighting measured chemical-shift changes in the region of lysine side chains between the free (green) and channel-bound states (red) of uniformly labeled KTX. Such shift changes are likely to occur as a result of specific toxin-channel interactions, as predicted from our MD analysis. It is important to note, however, that it cannot be excluded that this signal shift includes contributions from lysine side chains other than Lys27 in KTX. Figure 3B shows a region from

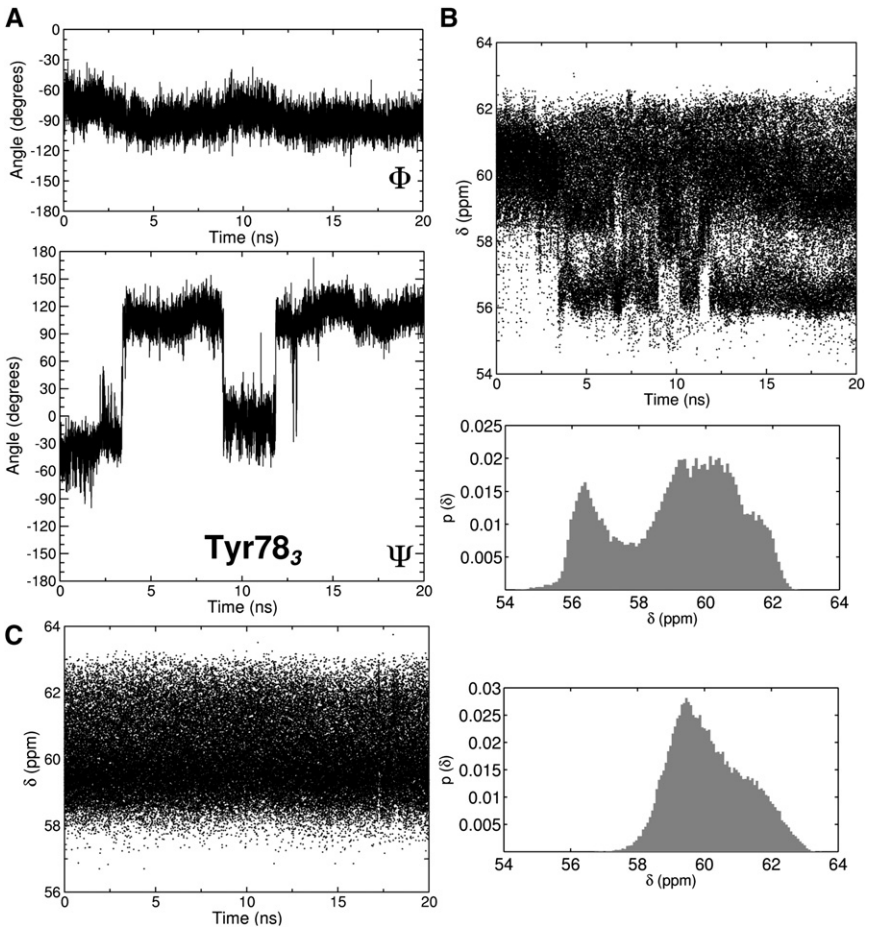

Figure 2. Conformational Change of the Backbone of Tyr78

(A) Change of the φ,ψ angles of Tyr78 in the selectivity filter in one subunit, caused by flipping into the cavity left by the Asp80 side chain flip in the MD simulation.

(B) Calculated chemical shift of the C_α of Tyr78 for all subunits. The rotation of the backbone of Tyr78 shown in (A) (t = 3.5–20 ns, with the exception of t = 9–12.5 ns) and, transiently, that of a second subunit (t = ~11 ns) results in a strongly shifted signal subpopulation and a bimodal distribution of chemical shifts.

(C) Reference simulation of the unbound state. The chemical shift remains unchanged and shows a single peak.

a carbon-carbon correlation spectrum of uniformly (^{15}N,^{13}C) labeled KcsA-Kv1.3 in the free state (green) and with bound KTX (red). The peak in the spectrum of the free channel at 61.7 ppm has been assigned to the Tyr78 C_α-C_β correlation (and two other α-helical Tyr residues [R.S., unpublished data]). It is seen to be split in the bound state (red), with the Tyr78 C_α signal shifted upfield by ~1.5 ppm. The magnitude and direction of the chemical-shift change are consistent with the SHIFTX prediction from our simulation trajectory within the accuracy limits of the program (Neal et al., 2003). The shifted peak at 60.2 ppm might either be an average over the flipped and nonflipped conformations of Tyr78, with the remaining peak originating from the other tyrosine groups, or the two peaks might directly represent the Tyr78 flipped and nonflipped conformations. The shift changes observed at Tyr78 in the simulation ensemble favorably agree with data from the ssNMR experiment.

KTX Binding to Kv1.3 Channels Is Sensitive to Their C-Type Inactivated State

Recently, Cordero-Morales et al. (2006a, 2006b) showed in studies combining electrophysiological measurements, mutant analysis, and crystallography that proton-dependent activation of the KcsA potassium channel is followed by an inactivation process at the selectivity filter similar to C-type inactivation. Conformational changes involving the Asp80-Glu71 pair apparently play an important role in this process (Cordero-Morales et al., 2006a, 2007). Mutation of Glu71 to alanine (E71A) allows Asp80 to fully flip out and prevents the channel from entering into the inactivated state (Cordero-Morales et al., 2006a). Since conformational changes associated with KTX:KcsA-Kv1.3 complex formation involve the Asp80-Glu71 pair, we hypothesized

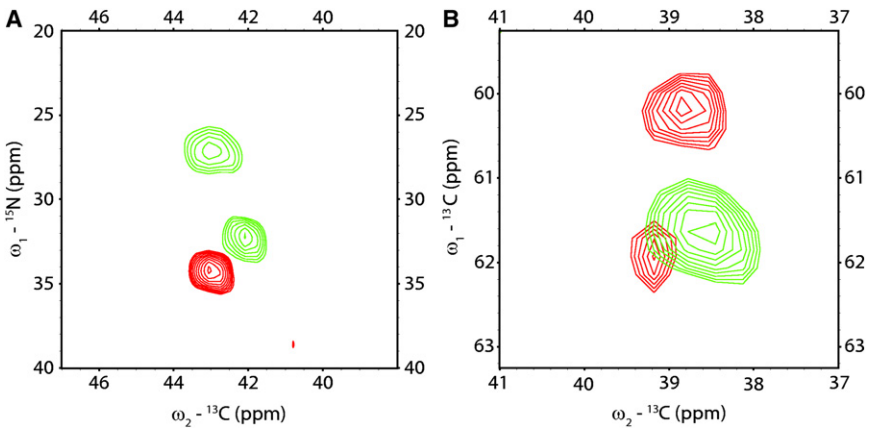

Figure 3. Sections of Two-Dimensional (^{15}N,^{13}C) and (^{13}C,^{13}C) ssNMR Correlation Spectra of KTX and KcsA-Kv1.3 in the Complexed and Free States

(A) Lysine NZ-CE region of two-dimensional (^{15}N,^{13}C) correlation spectra of free KTX (green) and KTX bound to KcsA-Kv1.3 (red).

(B) Tyrosine CA-CB region of two-dimensional (^{13}C,^{13}C) correlation spectra for the free KcsA-Kv1.3 potassium channel (green) and for KcsA-Kv1.3 complexed with KTX (red).

that C-type inactivation may reduce the KTX-binding affinity of K^+ channels. To study the influence of C-type inactivation on KTX binding, we chose the Kv1.3 channel, which binds KTX with very high affinity and readily enters into C-type inactivation. Kv1.3 channels were expressed in the *Xenopus* oocyte expression system. We used two pulse protocols, which differed in test pulse duration, to measure KTX inhibition of the Kv1.3 current. In the first protocol, we repeatedly depolarized from a holding potential of −80 mV for 50 ms to +60 mV at 10 s intervals. With this protocol, we measured KTX affinity for closed and opened Kv1.3 channels. The observed EC_{50} of 0.06 nM is in agreement with previous reports (Lange et al., 2006). In the second protocol, we used test pulse durations of 60 s, allowing the Kv1.3 channels to fully enter into C-type inactivation. As Figure 4 shows, this pulse protocol lowered the affinity of KTX for Kv1.3 20-fold (EC_{50} = 1.2 nM). The results suggest that C-type inactivation changes the KTX interaction surface. Consistent with this view, we found a 10-fold decrease in k_{on} values (0.0014 s^{-1} versus 0.01 s^{-1}).

KTX binding is favored by an activated state of the Kv channel, suggesting that C-type inactivation changes the interaction surface with KTX. The measured effect can be largely attributed to a decreased on rate of KTX binding. It is likely that KTX binding either induces recovery from inactivation of the K^+ channel or shifts the C-type activation/inactivation equilibrium toward the activated state. The alteration of the geometry of the upper region of the selectivity filter from Gly77 to Gly79 that was observed in the MD trajectory led to a significant widening of the channel entrance, and it allowed for a deeper insertion of the KTX Lys27 side chain (Figure 1C). We propose that KTX interacts with the charged side chain of Asp80 in KcsA-Kv1.3 and with the corresponding Asp402 in Kv1.3 (which is homologous to Kv1.2 Asp379). In addition, we suggest that KTX association alters the protonation state of Glu71, or shifts its equilibrium toward the deprotonated state in the KcsA-Kv1.3 channel chimera. This glutamate is replaced by valine in the voltage-gated channel subfamily (Long et al., 2005). The role of this group in KTX binding to Kv1.3 is therefore unclear, and it is possible that the Asp402 side chain is mainly responsible for the correlation between KTX binding and C-type inactivation in Kv1.3.

Heterogeneity of KTX-Bound States May Contribute to High Affinity

KTX binding might be expected to remove the degeneracy of the chemical shifts of the channel tetramers due to its nonsymmetric shape (Figure 5A). An intriguing observation made in the ssNMR experiment was that the channel displays overall four-fold symmetry in the complex, with only the KTX Lys27 possibly inducing asymmetric chemical-shift changes at Tyr78 in the selectivity filter. One possible explanation is structural heterogeneity in the bound states, i.e., an ensemble of tight structures formed after binding of KTX to the channel. Such an ensemble would average out further local breaches of symmetry in the tetramer, as long as Lys27 remains bound to the selectivity filter.

To test this hypothesis, we produced an ensemble of complexes from our MD structural model by using CONCOORD (de Groot et al., 1997). As constraints, we assumed that KTX Lys27 is inserted into the selectivity filter and that the side chains of Asp80 and Glu71 are charged, as in the MD simulations. We tested the stability of ten structural models in 10 ns MD simulations, introducing a wide variation in the position and orientation of bound KTX in the starting structures.

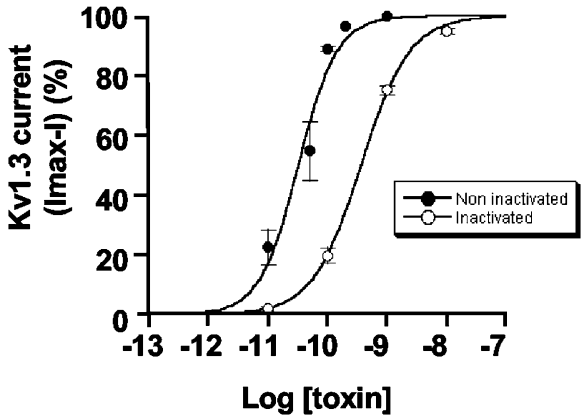

Figure 4. Binding of KTX to Kv1.3 Potassium Channels in the Non-Inactivated and Inactivated States

K^+ current through the Kv channels is plotted versus KTX concentration.

Most of the KTX molecules remained stably bound to KcsA-Kv1.3 in these simulations (Figure 5B). Further spontaneous backbone flips of Tyr78 were seen in the simulations, i.e., the situations are consistent with the local asymmetric change observed in ssNMR after KTX binding. This result suggests that an ensemble of toxin-bound states, rather than a single, complexed structure, may be formed by KTX binding to KcsA-Kv1.3. The conformational changes triggered by KTX association at Asp80 and Glu71 and the region between Gly77 and Gly79 of the selectivity filter may be sufficient to allow tight binding of KTX and channel blockade by Lys27.

It is important to note the computational constraint of investigating the complex on rather short timescales, which may lead to insufficient convergence of toxin-bound states. Also, other explanations are conceivable for observation of largely symmetric ssNMR signals, such as insufficient ssNMR signal resolution.

DISCUSSION

Our study provides a structural model for the chemical shift changes observed upon high-affinity binding of KTX to the chimeric potassium channel KcsA-Kv1.3. Due to their sharing of many important features, such as dependence on the same set of point mutations in the external pore vestibule, or sensitivity to external tetraethylammonium (TEA), a connection between the association of peptidic toxins and C-type inactivation was long assumed, but could not yet be clearly established by using low-affinity toxin peptides (Kurata and Fedida, 2006; Oliva et al., 2005; Koch et al., 2004). These conformational effects could thus far only be studied indirectly because of the lack of a high-resolution structural picture for both toxin binding and C-type inactivation (Kurata and Fedida, 2006).

Our MD results point to a structural similarity between the conformational changes due to KTX binding as measured by ssNMR and those elicited by recovery from C-type inactivation (Cordero-Morales et al., 2006a, 2006b, 2007). Electrophysiological measurements confirm this structural view functionally. The

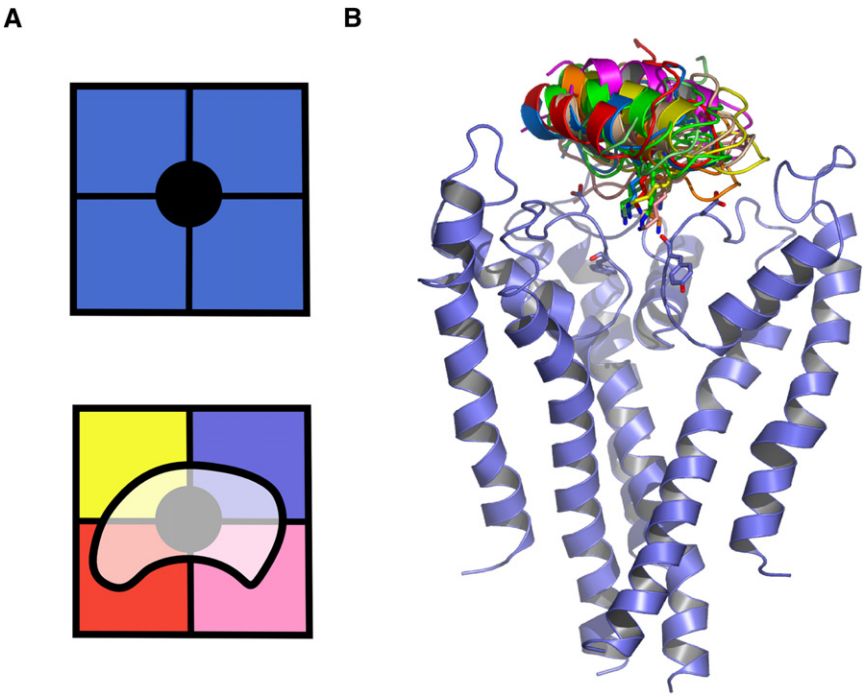

Figure 5. Heterogeneity Might Explain Preservation of the Four-Fold Symmetry in ssNMR

(A) Binding of asymmetric KTX should lead to a breach of symmetry in the ssNMR signals of the KcsA-Kv1.3 subunits, which was, however, only seen for the selectivity filter (see Figure 3).

(B) Heterogeneity in binding of KTX to KcsA-Kv1.3 within the 90° range might restore the overall four-fold symmetry after binding.

structural determinants of tight toxin association appear to be flipping of the Asp80 side chain and subsequent deep insertion of the Lys27 side chain after rotation of the Tyr78 backbone. In the KcsA-Kv1.3 channel chimera, a change in the protonation state of Glu71 is probably required. Both the rotation of Asp80 and the subsequent backbone flip around Tyr78 widen the entrance of the selectivity filter. Our study suggests that these conformational changes are sufficient to allow for an efficient KTX block of the channel, as we observe a heterogeneity of stable KTX:KcsA-Kv1.3 complexes consistent with the ssNMR data.

A similarly deformed structure of the selectivity filter region was observed in the crystal structure of the constitutively conductive conformation of the E71A KcsA mutant (Cordero-Morales et al., 2006a). The flipped Asp80 crystal structure exhibits a conformational change in the region of Tyr78 similar to the one we observed in our toxin-bound MD simulation: a rotation of the backbone that turns the carbonyl oxygen toward the cavity formed by the Asp80 side chain flip. A backbone flip of Val76 was also observed in the E71A KcsA crystal structure, which, however, cannot take place here because the charged side chain of Glu71 fills this region instead of the shorter alanine in the X-ray structure. Moreover, very recent results showed that the distance between Asp80 and Glu71 is indeed the major determinant of C-type inactivation in KcsA, with a larger distance favoring the activated state (Cordero-Morales et al., 2007), a finding that is clearly corroborated by our results.

We calculated the chemical shifts for the Tyr78 C_α signal of both the nonflipped and flipped crystal structures of the E71A KcsA crystal structure (Cordero-Morales et al., 2006a). The original high-resolution structure of conductive KcsA (Zhou et al., 2001) yields a calculated signal at $\delta = 60.5$ ppm. The nonflipped E71A KcsA structure, which is sequence identical to KcsA-Kv1.3 in the selectivity filter region, shows a calculated chemical shift of $\delta = 59.6$ ppm, which is insignificantly different given the accuracy limits of the SHIFTX program (Neal et al., 2003). The crystal structure of E71A KcsA has the Tyr78 flipped, which results in an expected Tyr78 C_α signal at $\delta = 56.8$ ppm. These values correspond almost perfectly to the chemical-shift change observed upon the Tyr78 backbone flip in our simulation (see Figure 2B), and they further support the structural picture derived from our MD simulations. The combination of ssNMR data with MD studies hence provides a powerful means by which to study structural alterations due to protein dynamics (Heise et al., 2005), even, as shown here, in the context of molecular interaction events in membranes.

The structural view of the KTX:KcsA-Kv1.3 pair represents a protein-protein interaction in which a conformational change upon binding increases the affinity significantly. Opening of the entrance region of the selectivity filter, together with the rotation of acidic side chains increasing the number of contacts with KTX, forms the basis for an intimate interaction of the toxin with the channel and, thus, a tight blockade of K^+ conduction.

EXPERIMENTAL PROCEDURES

Molecular Dynamics Simulations

An equilibrated simulation box of 241 palmitoyloleoylphosphatidylcholine (POPC) lipids and 10,129 water molecules was chosen as the starting configuration for the simulations. The channel was inserted by using the guidelines given by Faraldo-Gomez et al. (2002). The crystal structures of both 1K4C and 1K4D (Zhou et al., 2001) from the Protein Data Bank were investigated. Additional information concerning dihedral angles and distance constraints as measured by ssNMR was used (Lange et al., 2006). The Kv1.3 mutations were introduced into KcsA and optimized by using Whatif (Vriend, 1990). For the starting structure of the channel-KTX complexation simulation that was analyzed further, the crystal structure 1K4D (Zhou et al., 2001) for low K^+ concentration was taken and the backbone angles deduced from ssNMR (Lange et al., 2006) were imposed first, since the ssNMR experiment was performed under low K^+ conditions. All backbone angles were then released during the simulations. The parameters for POPC were taken from Berger et al. (1997); the OPLS-all-atom force field (Jorgensen et al., 1996) was used for the protein, and the solvent was described by the TIP4P water model (Jorgensen et al., 1983). All simulations were carried out by using the Gromacs simulation software, version 3.3 (Lindahl et al., 2001). Electrostatic interactions were calculated explicitly at a distance smaller than 1 nm, and long-range electrostatic interactions were calculated at every step by particle-mesh Ewald summation (Darden et al., 1993). Lennard-Jones interactions were calculated with a cutoff of 1 nm. All bonds were constrained by using the LINCS algorithm (Hess et al.,

1997), allowing for an integration time step of 2 fs. The simulation temperature was kept constant by weakly (τ = 0.1 ps) coupling the lipids, protein, and solvent separately to a temperature bath of 300 K. Likewise, the pressure was kept constant by weakly coupling the system to a pressure bath of 1 bar.

The ssNMR structure of KTX (1XSW in the PDB) (Lange et al., 2006) was added to the extracellular side of KcsA-Kv1.3, after extensive equilibration of the membrane system (5 ns) and enlarging the water box. The only assumption that was made concerning the starting configuration was to place KTX such that the experimentally determined contact surface roughly pointed toward the nearest membrane bilayer in the periodic system; no further restraints or biasing forces were applied during the setup and simulation. The final system comprised ~85,000 atoms with and ~56,000 atoms without added KTX. Simulation trajectories of 10–20 ns length were obtained. Chemical shifts were calculated with the SHIFTX program (Neal et al., 2003). For the flipped state of E71A KcsA, the entry 2ATK was taken from the PDB (Cordero-Morales et al., 2006a).

Solid-State NMR

Two-dimensional solid-state NMR experiments were conducted on a 14.1 T (^{1}H resonance frequency: 600 MHz) wide-bore instrument (Bruker Biospin, Germany) equipped with a 4 mm triple-resonance (^{1}H, ^{13}C, ^{15}N) MAS probe. All experiments were carried out at probe temperatures of −25 to −30°C by using an MAS rate of 9.375 kHz. Frequency-selective (^{15}N,^{13}C) polarization transfer for (^{13}C,^{13}C) correlation spectra was established under SPECIFIC-CP (Baldus et al., 1998) conditions (typically for a duration of 4 ms). For (^{15}N,^{13}C) correlation spectra, a conventional proton-driven spin diffusion scheme employing a longitudinal mixing time of 20 ms was used. ^{13}C resonances were calibrated by using adamantane as an external reference. The upfield resonance of adamantane was set to 31.47 ppm to allow for a direct comparison of the solid-state chemical shifts to solution-state NMR data. Accordingly, ^{15}N resonances were calibrated by using the tripeptide AGG as an external reference (Luca et al., 2001; Baldus et al., 1998).

Electrophysiology

The expression of Kv1.3 channels in *Xenopus* oocytes was measured 1 day after injection of Kv1.3 cRNA (50 ng/μl) in the two-electrode voltage-clamp configuration as described previously (Long et al., 2005). Bath solution was 80 mM NaCl, 2.0 mM KCl, 2.0 mM $CaCl_2$, 1.0 mM $MgCl_2$, 5.0 mM HEPES (adjusted to pH 7.5). Outward currents were elicited at room temperature from −80 mV holding potentials either to 50 ms or 50 s long test potentials at +60 mV, followed by 10 s intervals at −80 mV. KTX (10 pM–10 nM in bath solution containing 0.2% bovine serum albumine) was applied to skinned oocytes by bath perfusion. All experiments were repeated 3–6 times. The effects of toxin on Kv1.3 current amplitude were evaluated by using HEKA-PULSEFIT in combination with Kaleidagraph software.

ACKNOWLEDGMENTS

We thank Helmut Grubmüller for continuous support and fruitful discussions, David Wishart for providing the SHIFTX program, and Dutch Top Institute Pharma for financial support. R.S. thanks the graduate school 782 "Spectroscopy and Dynamics of Molecular Coils and Aggregates" of the German Research Council (DFG) for a Ph.D. fellowship. G.V. acknowledges The Netherlands Bioinformatics Centre, a subsidiary of The Netherlands Genomic Initiative, and BioSapiens, funded by the European Commission within its FP6 Programme, under the thematic area "Life Sciences, Genomics and Biotechnology for Health," contract number LSHG-CT-2003-503265, for financial support.

Received: October 17, 2007
Revised: January 30, 2008
Accepted: January 31, 2008
Published: May 6, 2008

REFERENCES

Aiyar, J., Withka, J.M., Rizzi, J.P., Singleton, D.H., Andrews, G.C., Lin, W., Boyd, J., Hanson, D.C., Simon, M., Dethlefs, B., et al. (1995). Topology of the pore-region of a K^+ channel revealed by the NMR-derived structures of scorpion toxins. Neuron *15*, 1169–1181.

Åqvist, J., and Luzhkov, V. (2000). Ion permeation mechanism of the potassium channel. Nature *404*, 881–884.

Baldus, M., Petkova, A.T., Herzfeld, J., and Griffin, R.G. (1998). Backbone and side chain assignment strategies for multiply labeled membrane peptides and proteins in the solid state. Mol. Phys. *95*, 1197–1207.

Berger, O., Edholm, O., and Jähnig, F. (1997). Molecular dynamics simulations of a fluid bilayer of dipalmitoylphosphatidylcholine at full hydration, constant pressure, and constant temperature. Biophys. J. *72*, 2002–2013.

Bernèche, S., and Roux, B. (2001). Energetics of ion conduction through the K^+ channel. Nature *414*, 73–77.

Bernèche, S., and Roux, B. (2002). The ionization state and the conformation of Glu-71 in the KcsA K^+ channel. Biophys. J. *82*, 772–780.

Bucher, D., Guidoni, L., and Rothlisberger, U. (2007). The protonation state of the Glu-71/Asp-80 residues in the KcsA potassium channel. A first-principles QM/MM molecular dynamics study. Biophys. J. *93*, 2315–2324.

Choi, H., and Heginbotham, L. (2004). Functional influence of the pore helix glutamate in the KcsA K^+ channel. Biophys. J. *86*, 2137–2144.

Cordero-Morales, J.F., Cuello, L.G., Zhao, Y., Jogini, V., Cortes, D.M., Roux, B., and Perozo, E. (2006a). Molecular determinants of gating at the potassium channel selectivity filter. Nat. Struct. Mol. Biol. *13*, 311–319.

Cordero-Morales, J.F., Cuello, L.G., and Perozo, E. (2006b). Voltage-dependent gating at the KcsA selectivity filter. Nat. Struct. Mol. Biol. *13*, 319–322.

Cordero-Morales, J.F., Jogini, V., Lewis, A., Vásquez, V., Cortes, D.M., Roux, B., and Perozo, E. (2007). Molecular driving forces determining potassium channel slow inactivation. Nat. Struct. Mol. Biol. *14*, 1062–1069. Published online October 7, 2007. 10.1038/nsmb1309.

Darden, T., York, D., and Pedersen, L. (1993). Particle mesh Ewald – an *Nlog(N)* method for Ewald sums in large systems. J. Chem. Phys. *98*, 10089–10092.

de Groot, B.L., van Aalten, D.M., Scheek, R.M., Amadei, A., Vriend, G., and Berendsen, H.J. (1997). Prediction of protein conformational freedom from distance constraints. Proteins *29*, 240–251.

Eriksson, M.A.L., and Roux, B. (2002). Modeling the structure of Agitoxin in complex with the Shaker K^+ channel: a computational approach based on experimental distance restraints extracted from thermodnamic mutant cycles. Biophys. J. *83*, 2595–2609.

Faraldo-Gomez, J.D., Smith, G.R., and Sansom, M.S.P. (2002). Setting up and optimization of membrane protein simulations. Eur. Biophys. J. *31*, 217–227.

Frederick, K.K., Marlow, M.S., Valentine, K.G., and Wand, A.J. (2007). Conformational entropy in molecular recognition by proteins. Nature *448*, 325–329.

Garcia, M.L., Gao, Y.D., McManus, O.B., and Kaczorowski, G.J. (2001). Potassium channels: from scorpion venoms to high resolution structure. Toxicon *39*, 739–748.

Goh, C.S., Milburn, D., and Gerstein, M. (2004). Conformational changes associated with protein-protein interactions. Curr. Opin. Struct. Biol. *14*, 104–109.

Heise, H., Luca, S., de Groot, B.L., Grubmüller, H., and Baldus, M. (2005). Probing conformational disorder in neurotensin by two-dimensional solid-state NMR and comparison to molecular dynamics simulations. Biophys. J. *89*, 2113–2120.

Hess, B., Bekker, H., Berendsen, H.J.C., and Fraaije, J.G.E.M. (1997). LINCS: a linear constraint solver for molecular simulations. J. Comput. Chem. *18*, 1463–1472.

Hidalgo, P., and MacKinnon, R. (1995). Revealing the architecture of a K^+ channel pore through mutant cycles with a peptide inhibitor. Science *268*, 307–310.

Hille, B., Armstrong, C.M., and MacKinnon, R. (1999). Ion channels: from idea to reality. Nat. Med. *5*, 1105–1109.

Jorgensen, W.L., Chandrasekhar, J., Madura, J.D., Impey, R.W., and Klein, M.L. (1983). Comparison of simple potential functions for simulating liquid water. J. Chem. Phys. *79*, 926–935.

Jorgensen, W.L., Maxwell, D.S., and Tirado-Rives, J. (1996). Development and testing of the OPLS-AA force field on conformational energetics and properties of organic liquids. J. Am. Chem. Soc. *118*, 11225–11236.

Koch, E.D., Olivera, B.M., Terlau, H., and Conti, F. (2004). The binding of κ-conotoxin PVIIA and fast C-type inactivation of Shaker K^+ channels are mutually exclusive. Biophys. J. *86*, 191–209.

Kurata, H.T., and Fedida, D. (2006). A structural interpretation of voltage-gated potassium channel inactivation. Prog. Biophys. Mol. Biol. *92*, 185–208.

Lange, A., Giller, K., Hornig, S., Martin-Eauclaire, M.F., Pongs, O., Becker, S., and Baldus, M. (2006). Toxin-induced conformational changes in a potassium channel revealed by solid-state NMR. Nature *440*, 959–962.

Lindahl, E., Hess, B., and van der Spoel, D. (2001). GROMACS 3.0: a package for molecular simulation and trajectory analysis. J. Mol. Model. *7*, 306–317.

Long, S.B., Campbell, E.B., and MacKinnon, R. (2005). Crystal structure of a mammalian voltage-dependent Shaker family K^+ channel. Science *309*, 897–903.

Luca, S., Filippov, D.V., van Boom, J.H., Oschkinat, H., de Groot, H.J.M., and Baldus, M. (2001). Secondary chemical shifts in immobilized peptides: a qualitative basis for structure refinement under magic angle spinning. J. Biomol. NMR *20*, 325–331.

Luzhkov, V.B., and Åqvist, J. (2000). A computational study of ion binding and protonation states in the KcsA potassium channel. Biochim. Biophys. Acta *1481*, 360–370.

MacKinnon, R., Cohen, S.L., Kuo, A., Lee, A., and Chait, B.T. (1998). Structural conservation in prokaryotic and eukaryotic potassium channels. Science *280*, 106–109.

Neal, S., Nip, A.M., Zhang, H., and Wishart, D.S. (2003). Rapid and accurate calculation of ^1H, ^{13}C and ^{15}N chemical shifts. J. Biomol. NMR *26*, 215–240.

Oliva, C., Gonzalez, V., and Naranjo, D. (2005). Slow inactivation in voltage gated potassium channels is insensitive to the binding of pore occluding peptide toxins. Biophys. J. *89*, 1009–1019.

Ranganathan, R., Lewis, J.H., and MacKinnon, R. (1996). Spatial localization of the K^+ channel selectivity filter by mutant cycle-based structure analysis. Neuron *16*, 131–139.

Roux, B. (2005). Ion conduction and selectivity in K^+ channels. Annu. Rev. Biophys. Biomol. Struct. *34*, 153–171.

Shrivastava, I.H., and Sansom, M.S. (2000). Simulations of ion permeation through a potassium channel: molecular dynamics of KcsA in a phospholipid bilayer. Biophys. J. *78*, 557–570.

Tobi, D., and Bahar, I. (2005). Structural changes involved in protein binding correlate with intrinsic motions of proteins in the unbound state. Proc. Natl. Acad. Sci. USA *102*, 18908–18913.

Vriend, G. (1990). WHAT IF – a molecular modeling and drug design program. J. Mol. Graph. *8*, 52–56.

Yellen, G. (2005). The voltage-gated potassium channels and their relatives. Nature *419*, 35–42.

Zhou, Y., Morais-Cabral, J.H., Kaufmann, A., and MacKinnon, R. (2001). Chemistry of ion coordination and hydration revealed by a K^+ channel-Fab complex a 2.0 Å resolution. Nature *414*, 43–48.

